

Phase Inversion Process to Prepare Quasi-Solid-State Electrolyte for the Dye-Sensitized Solar Cells

Jing Zhang, Hongwei Han, Sheng Xu, Sujuan Wu, Conghua Zhou, Ying Yang, Xingzhong Zhao

Department of Physics, Key Laboratory of Acoustic and Photonic Materials and Devices of Ministry of Education, Wuhan University, Wuhan 430072, China

Received 28 June 2006; accepted 31 January 2008

DOI 10.1002/app.28208

Published online 17 April 2008 in Wiley InterScience (www.interscience.wiley.com).

ABSTRACT: A quasi-solid-state electrolyte for the dye-sensitized solar cells was prepared following the phase inversion process. The microporous polymer electrolyte based on poly(vinylidene fluoride-co-hexafluoropropylene) (P(VDF-HFP)) hybrid with different amount of TiO₂ nanoparticles were prepared. The surface morphologies, the differential scanning calorimetry, and the ionic conductivity of the microporous polymer electrolyte were tested and analyzed. The results indicated that the microporous polymer electrolyte with TiO₂ nanoparticles modification exhibited better ionic conductivity compared with the original P(VDF-HFP) polymer electrolyte. The optimal ionic con-

ductivity of 0.8 mS cm⁻¹ is obtained with the 30 wt % TiO₂ nanoparticles modification. When assembled with the 30 wt % TiO₂ nanoparticles modified quasi-solid-state electrolyte, the dye-sensitized TiO₂ nanocrystalline solar cell exhibited the light to electricity conversion efficiency of 2.465% at light intensity of 42.6 mW cm⁻², much better than the performance of original P(VDF-HFP) microporous polymer electrolyte DSSC. © 2008 Wiley Periodicals, Inc. *J Appl Polym Sci* 109: 1369–1375, 2008

Key words: dye-sensitized solar cells; quasi-solid-state; microporous polymer electrolyte; phase inversion process

INTRODUCTION

Dye-sensitized solar cells (DSSCs) have promised to provide a “leapfrog” in solar cell cost effectiveness and the field has attracted an increasing number of academic and industrial research teams, especially 10% efficient dye sensitized solar cells were demonstrated.^{1–6} The DSSCs provide a technically and economically credible alternative concept to conventional *p-n* junction photovoltaic device.⁷ Recently, there is a tendency to replace the liquid electrolyte with the solid or quasi-solid-state electrolyte, considering the leakage and evaporation of the liquid electrolyte. Many efforts, for example, using P-type semiconductor, hole conductor, and polymeric or gel materials incorporating triiodide/iodide as a redox couple were introduced to substitute the liquid electrolyte.^{8–11} Research groups focus on improving the conductivity and the interface connection between solid or quasi-solid-state electrolyte and the semiconductor.¹² Moreover, numerous investigations of solid or quasi-solid-state electrolytes have been carried out with special emphasis on applications to lithium batteries.^{10,13}

Generally, two methods of preparing polymer electrolytes for lithium batteries have been employed: (1) dissolution of the polymer host, lith-

ium salt, and plasticizers in a nonvolatile solvent, which is evaporated to form films. (2) The second method, called phase inversion or activation process, involves soaking the polymer film in an electrolytic solution.¹⁴ The second method, which was first disclosed and patented by Telcordia Technologies (formerly Bellcore), has been widely studied and used in the lithium batteries as an effective way to prepare laminated Li-ion plastic batteries.^{15,16}

A lot of research groups have studied the solid or quasi-solid state electrolyte for dye sensitized solar cells using method. (1) In this article, the quasi-solid-state electrolyte is prepared following the phase inversion process for the dye sensitized solar cells. And the effect of addition of TiO₂ nanoparticles in the polymer matrix is checked.

Series of porous polymer membranes filled with various amount of TiO₂ nanoparticles were prepared by the phase inversion process. The commercialized P25 TiO₂ nanoparticles (Degussa AG, Germany, 20–30 nm) are used as the inorganic fillers to improve the membrane's ionic conductive property. The effect of TiO₂ nanoparticles on the crystallinity of the polymer membrane and the ionic conductivity of polymer electrolyte are investigated. The highest ionic conductivity reached at 0.8 mS cm⁻¹ when the TiO₂ nanoparticles was added at 30 wt % of P(VDF-HFP). The dye sensitized TiO₂ nanocrystalline cell device assembled with the 30 wt % TiO₂ nanoparticles modified quasi-solid-state electrolyte showed improved light to electricity conversion efficiency

Correspondence to: X.-Z. Zhao (xzzhao@whu.edu.cn).

compared with the original polymer electrolyte DSSC without TiO₂ nanoparticles modification under 42.6 mW cm⁻² light irradiation.

EXPERIMENTAL

Quasi-solid-state electrolyte preparation

Followed by phase inversion process, P(VDF-HFP) (Kynar 2801, Elf Atochem, North America) was chosen as the polymer, acetone was used as a solvent and ethanol as the nonsolvent. About 10 wt % P(VDF-HFP) was dissolved in 2 : 1 v/v mixture of acetone and ethanol, stirred vigorously in the water bath condition at 50°C until the polymer dissolved completely. Then a proper amount of P25 TiO₂ nanoparticles (Degussa, German) was added to the slurry and the stirring was continued for 4 h to mix the materials uniformly. To examine the effect of inorganic particle on the physical–chemical property of the membrane, the weight ratio of the P25 nanoparticles to P(VDF-HFP) was varied as 0, 10, 20, 30, and 40 wt %.

The resulting slurry was then doctor bladed onto the glass slide. After placed in the air for several minutes, the membranes were baked in the Bench-Top Type Temperature and Humidity Chamber (Espec cop, Japan) at 75°C for about 4 h, allowing the evaporation of the acetone and the ethanol. For ionic conductivity measurement, the prepared membranes were soaked in the electrolyte solution containing 0.05M of I₂, 0.5M of LiI, and 0.5M of 4-*tert*-butylpyridine in Propylene Carbonate. This process was called electrolyte activation.¹⁵

Characterization of the porous polymer membrane

The surface morphology of the membranes with different P25 content was studied using Atomic force microscope (AFM, SPM-9500J3). The square average roughness (RMS) of the measured surfaces were also provided.

The X-ray diffraction (XRD) of the polymer electrolyte membranes was carried out on a Bruker D8 advance X-ray diffractometer using Cu K α radiation at 40 kV and 20 mA in the region of $2\theta = 2\text{--}65^\circ$.

Differential scanning calorimetry (DSC) thermograms of the polymer electrolyte membranes were measured with a NETZSCH DSC 200PC (German) at heating rate of 10°C min⁻¹ under nitrogen atmosphere and in the temperature range of 40–200°C.

The liquid uptake of the microporous polymer membrane

After different content TiO₂ nanoparticles-modified microporous polymer membranes were prepared,

the film samples were weighted and marked as W_0 ; then, the microporous films were immersed in PC (propylene carbonate) for 12 h, after removed the excess PC, the films were weighted again and marked as W_1 . The electrolyte uptake was defined as: $\Delta w\% = (W_1 - W_0)/W_0 \times 100\%$.

Ionic conductivity measurement

The activated membrane was mounted in a clamp designed by us, where the membrane can be clamped tightly between two thermally gilded copper cylinders, which serve as the electrode (the electrode area is 0.132 cm²). The temperature dependence of the conductivity of the polymer membrane was measured in Bench-Top Type Temperature and Humidity Chamber with temperature ranging from -10 to 80°C at intervals of 10°C. All the impedance response measurements were carried out by Agilent 4294A precision impedance analyzer (USA), a perturbation voltage of 500 mV was applied over the frequency range 40 Hz–1 MHz.^{17,18}

Assembly of the quasi-solid-state DSSC

A hybrid TiO₂ photoanode was fabricated on transparent conducting oxide (TCO, Asahi Glass, Japan) substrates following the method according to the literature.¹⁹

A compact and transparent TiO₂ layer was first deposited on a conducting glass substrate (SnO₂: F, Asahi Glass, Japan) by DC magnetron sputtering, then a nanocrystalline TiO₂ layer (thickness: about 8 μ m) was prepared by doctor-blade technique. The TiO₂ nanoparticles used here is the commercialized P25 nanoparticles, which were used for the TiO₂ photoanodes preparation and modification of the quasi solid electrolyte. The thickness of the TiO₂ photoanode was measured by a nanostep instrument (Form Talysurf S4C, Taylor Hobson). After sintering at 450°C for 30 min and cooling down to 80°C, the TiO₂ photoanodes were dye coated by immersing them into a dye solution of 0.5 mM N719 (Ruthenium 535 bisTBA, Dyesol, Australia) in dry ethanol at 50°C for at least 12 h. After the sensitization, the microporous polymer membrane was assembled onto it following the process presented in Quasi-Solid-State Electrolyte Preparation section, then soaked it in electrolyte solution for 24 h. For measurement, a platinized SnO₂: F glass which serves as the counter electrode was placed on the top and squeezed against the microporous polymer electrolyte by a clamp. A mask was used to control the effective cell area to be 0.5 cm².

Photoelectrochemical measurement

The photocurrent-density/voltage curves were measured in a two-electrode system under the light of xenon lamp using Keithley Model 2400 Digital Source Meter unit (USA). A 500 W xenon lamp served as the light source in conjunction with filters cutting off the UV (< 400 nm) and IR (> 800 nm) components of the light. The light intensity was obtained using the irradiatometer made in China. The energy conversion efficiencies reported here are overall yields, which are uncorrected for losses due to light absorption and reflection by the conducting glass support.

RESULTS AND ANALYSIS

According to phase inversion process, microporous structured membrane is prepared by solvent casting from a solution of the polymer (usually poly(vinylidene fluoride-co-hexafluoropropylene), P(VDF-HFP) in short) in a mixture of its solvent and nonsolvent in the presence of a finely divided filler, and by taking advantage of a differential evaporation rate and various solvation properties of the two solvents.¹⁴ The microporous structured membrane, which can adsorb and retain a large amount of the electrolyte solution, shows it is a good matrix for ionic conducting.²⁰

Recently, poly(vinylidene fluoride-co-hexafluoropropylene) copolymers, which has the lower crystallinity and glass transition temperature than pure PVDF, have been used as a main substance of polymer electrolyte in the most commonly commercialized plastic lithium-ion batteries (PLiON™). On the other hand, the addition of inorganic fillers such as silica (SiO₂) or Al₂O₃ nanoparticles to the polymer electrolyte results in the enhancement of physical strength as well as the increase in the absorption level of electrolytes solution. The absorption level is the ability of the prepared microporous polymer membrane to trap the liquid electrolyte.^{15,16} In addition to these effects, they act as a solid plasticizer hindering the crystallization of the polymer and reorganizing of polymer chains by Lewis acid-base effect so the ionic conductivity is improved.^{15,21,22} Here, the commercialized P25 TiO₂ nanoparticles were added in the P(VDF-HFP) polymer matrix for its low cost and nontoxic. Properties of different amount of TiO₂ nanoparticles-modified microporous membranes are investigated, and the properties further influenced the performance of the DSSC.

Surface morphologies of the hybrid P(VDF-HFP) polymer membranes

Ions migrate in two ways in the microporous electrolyte: (1) the ions move in the swollen phase of the

polymer membrane, and (2) move in the liquid electrolyte retained by the micropores.^{21,23,24} The former is slow transport while the latter is fast. In the microporous polymer electrolyte, the main conductive mechanism is the (2). The ions migrate not only in gel electrolyte but also in liquid electrolyte, so the pore structure which can retain large amount of liquid electrolyte influences the ionic conductivity in larger. In the dye sensitized solar cell, the redox electrolyte which can regenerate the original state of the dye and conduct the electron from the counter electrode, is mainly retained in the pore structure. The fine and uniform porous membranes is considered useful for the back and forth movement of the redox couple.²⁵

AFM top-view images (Fig. 1) reveal that the morphologies of the polymer membranes with different TiO₂ ratio are microporous and the square average roughness values are indicated in Table I. The images indicated that phase inversion process is a well-known technology for making microporous polymer membrane and the addition of TiO₂ nanoparticles changes the membrane's morphology. The membrane without TiO₂ nanoparticles shows only the microporous and rough structure [Fig. 1(a)]. With increasing the TiO₂ ratio, the surface of the polymer membrane becomes more porous [Fig. 1(b-e)] and the surface roughness factor (square average roughness, RMS in short) increases. Table I exhibited the RMS of the P(VDF-HFP) membranes filled with different content of TiO₂ nanoparticles. The square average roughness is defined as: the root mean square value of the surface roughness profile from the center line within the measuring length. The corresponding expression is $RMS = \left(\frac{Y_1^2 + Y_2^2 + Y_3^2 + \dots + Y_n^2}{N} \right)^{1/2}$.²⁶

Comparing with the RMS = 51.73 nm of the original polymer membrane, the RMS reached maximum value of 139.304 nm at 30 wt % TiO₂ content, and further dropped to 87.073 nm at 40 wt % TiO₂ content. The images and the RMS suggested that the morphologies with the TiO₂/P(VDF-HFP) weight ratio of 30 wt % have fine and uniform pore size and more rough surface, when soaked in the liquid electrolyte, the pores are believed to be good to the ionic conductivity. The electrolyte uptake was performed and the results were also exhibited in Table I. The results exhibited that TiO₂ nanoparticles modification improved the liquid uptake content, and 30 wt % TiO₂ nanoparticles modified microporous membrane exhibited better electrolyte uptake.

It is believed that TiO₂ nanoparticles, which is capable of forming hydrogen bonds with the alcohol molecules, is well-wetted by the latter and is therefore concentrated in the phase-separated alcohol droplets which give origin to the pores. During

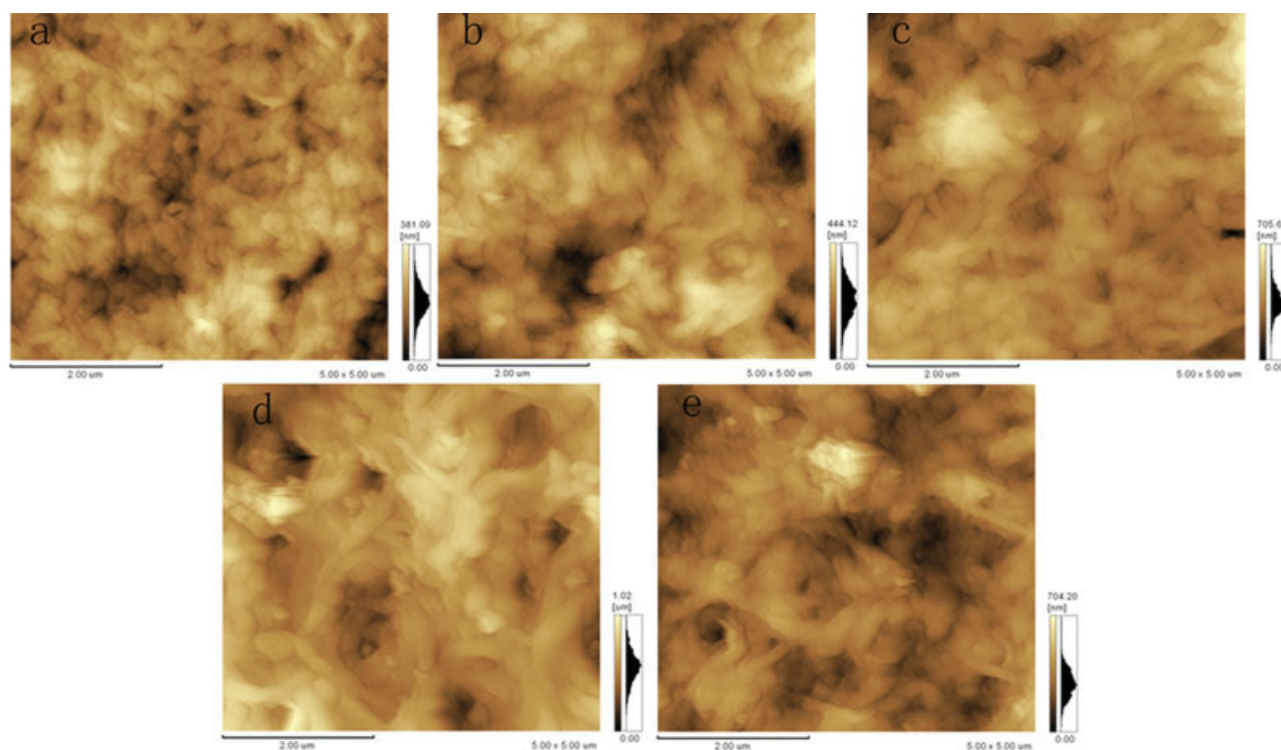


Figure 1 AFM top-view images of P(VDF-HFP) membrane filled with different weight contents of TiO₂ nanoparticles: (a) 0%; (b) 10 wt %; (c) 20 wt %; (d) 30 wt %; (e) 40 wt %. [Color figure can be viewed in the online issue, which is available at www.interscience.wiley.com.]

acetone evaporation, the nanoparticles are fixed in the polymer matrix and create the pores. Such a particular structure is expected to enhance the mechanical stability and increasing the wetting ability of the electrolyte, so the electrolyte uptake was improved.¹⁴ Whereas too much TiO₂ nanoparticles are easy to aggregate, further decrease the pore size and the electrolyte uptake, which cannot give room to the ionic movement.

XRD analysis of TiO₂ nanoparticles modified P(VDF-HFP) polymer membranes

The XRD patterns for P(VDF-HFP) composite polymer membranes are shown in Figure 2. At low TiO₂ content, the film shows characteristic crystallinity peaks of P(VDF-HFP) ($2\theta \approx 17, 19, 38^\circ$ for PVDF α -

phase crystals).²⁷ The peaks at $2\theta = 25.5, 38.67, 48.29,$ and 55.35° are corresponding to, (101), (112) (200), and (211) planes of anatase TiO₂ nanoparticles; the peaks at $2\theta = 27.45, 36.11, 54.22,$ and 62.89° are corresponding to (110), (101), (211), and (002) planes of rutile-phase TiO₂ nanoparticles. With the content of the TiO₂ nanoparticles increase, the characteristic crystallinity peaks of both rutile and anatase TiO₂ nanoparticles increase. However the crystallinity of the polymer membrane decreases clearly with the increase of the TiO₂ nanoparticles. The information

TABLE I

The Square Average Roughness (RMS) and the Liquid Uptake of the P(VDF-HFP) Membranes Filled with Different Content of TiO₂ Nanoparticles

TiO ₂ (wt %)	0	10%	20%	30%	40%
RMS (nm)	51.73	69.6	83.529	139.304	87.073
$\Delta W\%$ (*100%)	1.20	1.38	1.82	2.74	1.25

The RMS data were obtained from the AFM measurement.

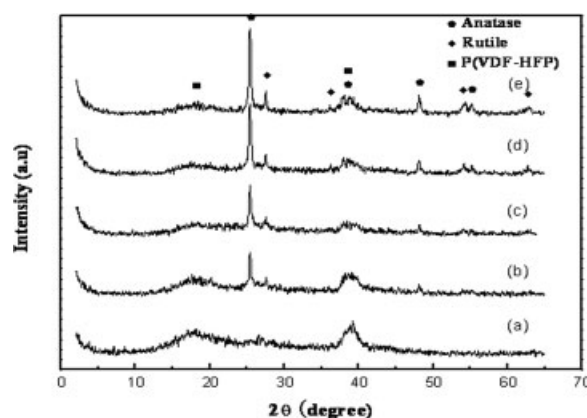


Figure 2 XRD patterns for the composite polymer membranes filled with various contents of TiO₂ nanoparticles. (a) 0%; (b) 10 wt %; (c) 20 wt %; (d) 30 wt %; (e) 40 wt %.

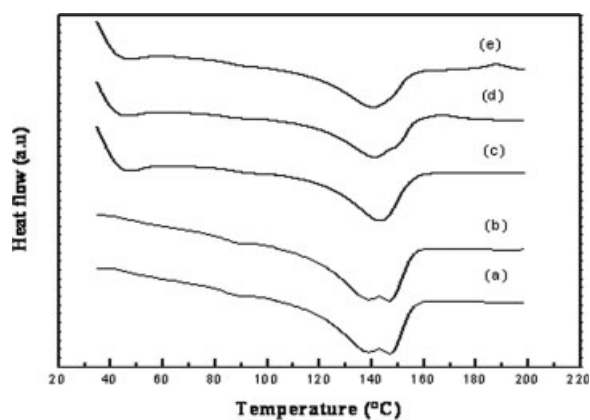


Figure 3 DSC curves of P(VDF-HFP) membranes filled with different amounts of TiO₂ nanoparticles. (a) 0%; (b) 10 wt %; (c) 20 wt %; (d) 30 wt %; (e) 40 wt %.

of characteristic crystallinity peaks of P(VDF-HFP) and TiO₂ all can also be obtained from Figure 2. The addition of the nanoparticles changed the crystallinity of P(VDF-HFP) clearly. The crystallinity of polymer chains maybe hindered by the interaction of the Lewis acid groups ceramics (e.g., the —OH groups on the titanic oxide surface) with the polar groups (e.g., the -F atoms of the polymer chains). As a result, the degree of crystallization of polymer matrix decreases with the addition of nanoparticles. Moreover, the interaction can stabilize the amorphous structure and enhance the ionic conductivity of the polymer electrolyte.^{21,22}

DSC thermograms of TiO₂ nanoparticles modified P(VDF-HFP) polymer membranes

The DSC thermograms of the P(VDF-HFP) composite polymer membranes are shown in Figure 3. The crystallinity of polymer membrane is calculated following eq. (1) from the DSC curves of polymer membranes:

$$X_c = (\Delta H_m / \Delta H_m^\phi) \times 100\% \quad (1)$$

where, ΔH_m^ϕ is the crystalline melting heat of pure α -PVDF, 104.7 J/g, ΔH_m the heat of fusion for P(VDF-HFP) membrane, respectively.²⁷ The data of ΔH_m , T_m and the crystallinity (X_c) are shown in Table II.

The DSC thermograms indicated that the amount of TiO₂ nanoparticles influences slightly on the crystalline melting temperature (T_m). However, the crystallinity ($X_c/\%$) and the heat of fusion for P(VDF-HFP) membrane (ΔH_m) decrease with the increase of the amount of TiO₂ nanoparticles within polymer membranes. The data also showed the effect of the nanoparticles on the polymer membrane system: the addition of TiO₂ nanoparticles makes the polymer chain reorganized that the crystallinity of the original P(VDF-HFP) decreased.²²

From the XRD and DSC analysis of the TiO₂ nanoparticles modified P(VDF-HFP) polymer membrane, it can be concluded that the crystallinity of the original P(VDF-HFP) decreased after the TiO₂ nanoparticles modification. The decreased crystallinity indicated the amorphous phase is increased after the TiO₂ nanoparticles modification. When the polymer membrane immersed in the electrolyte, the amorphous phase which might swollen the electrolyte can help improve the ionic movement.

Ionic conductivity of the microporous polymer electrode

For composite polymer electrolyte dye sensitized solar cell device, the overall solar to energy conversion efficiency is heavily dependent upon the mobility of the redox couple and consequently on the ionic conductivity of the polymer electrolyte.²⁸ The effect of the nanoparticles on the membranes' ionic conductivity ($T = 323$ K) is shown in Figure 4. And the inner figure is the Nyquist plots of the P(VDF-HFP) microporous membranes filled with different content of TiO₂ nanoparticles. The Nyquist plots are not the half-circle like for the low frequency is not low enough. The ionic conductivity σ of the membranes is calculated following the eq. (2):

$$\sigma = L/AR_b \quad (2)$$

where L is the thickness of the polymer electrolyte membrane and A is the area of the electrode. The resistance (R_b) was taken at the inflection point of the Nyquist plot in Figure 4.^{21,22}

From Figure 4, an increase of the ionic conductivity is observed when adding the TiO₂ nanoparticles in the polymer matrix. The ionic conductivity became outstanding of 0.8 mS cm⁻¹ when the matrix hybrid with 30 wt % TiO₂ nanoparticles, which is nearly 2.5 times larger than the original polymer matrix. The increase of ionic conductivity may be due to the formation of fine porous structure and the decreased crystallinity with the addition of 30 wt % TiO₂ nanoparticles.

Figure 5 exhibits ionic conductivity of the membranes varied with the temperature changing from

TABLE II
The Melting Temperature (T_m), the Heat of Fusion (ΔH_m) and the Crystallinity (X_c) of P(VDF-HFP) Membranes Filled with Different Content of TiO₂ Nanoparticles

TiO ₂ (wt %)	$T_m/^\circ\text{C}$	$\Delta H_m/\text{J g}^{-1}$	$X_c/\%$
0	143.1	48.5	46.3
10	139.7	39.5	37.7
20	143.1	38.57	36.8
30	141.3	31.75	30.3
40	140.4	30.82	29.4

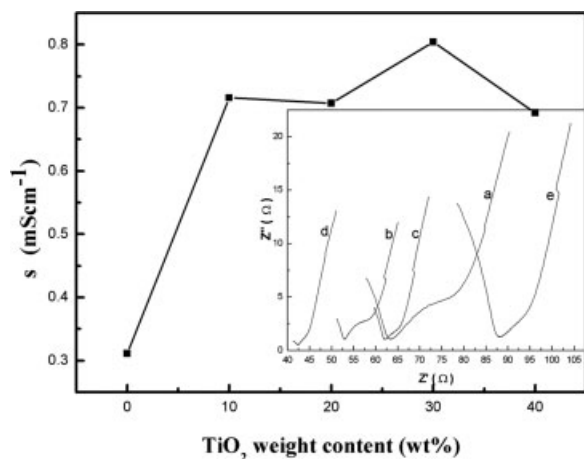


Figure 4 The effect of TiO₂ nanoparticle on the ionic conductivity of the microporous polymer electrolyte at $T = 323$ K. The inner figure is the Nyquist plots of the microporous polymer electrolyte with different TiO₂ nanoparticles content. (a) 0 wt %; (b) 10 wt %; (c) 20 wt %; (d) 30 wt %; (e) 40 wt %.

–10 to 80°C. The Arrhenius equation can fine describe the conductivity-temperature behavior of the liquid and polymer gel electrolytes:

$$\sigma(T) = A \exp(-E_a/RT) \quad (3)$$

where E_a is the activation energy, a is a constant and T is the absolute temperature.¹⁷

The temperature dependence of the microporous polymer electrolyte's ionic conductivity is suggested that the ionic conductivity increases with the increase of temperature. The conductivity of the membranes verified from 10^{-5} to 10^{-3} S cm⁻¹ for the temperature ranging from –10 to 80°C. Of all the membranes with different TiO₂ nanoparticles content, the membrane with the TiO₂ content of

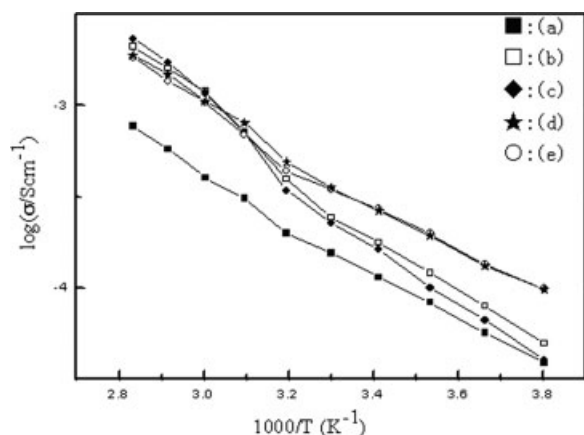


Figure 5 The membrane ionic conductivity dependence of the temperature ranging from –10 to 80°C. (a) TiO₂ nanoparticles content 0%; (b) 10 wt %; (c) 20 wt %; (d) 30 wt %; (e) 40 wt %.

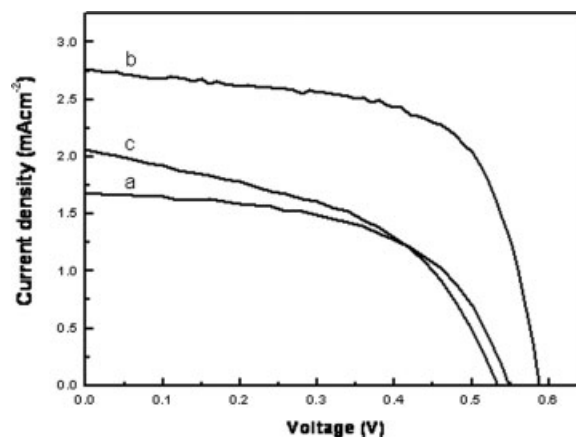


Figure 6 Photocurrent density-voltage characteristics of N719-sensitized nanocrystalline TiO₂ film solar cells using P(VDF-HFP)/TiO₂ membrane electrolyte and origin P(VDF-HFP) membrane. (a) 0 wt % TiO₂ nanoparticles content, (b) 30 wt %, (c) 40 wt % Conditions: temperature, ambient temperature; effective area, 0.5cm²; solar irradiance, 42.6 mW cm⁻².

30 wt % shows the optimal conductivities over the temperature range.

Photocurrent density–voltage characteristics of the as prepared solar cell

Photocurrent density–voltage characteristics of N719-sensitized nanocrystalline TiO₂ film solar cells using original P(VDF-HFP), 30 and 40 wt % TiO₂ nanoparticles hybrid polymer membrane electrolyte were measured at Xe lamp simulated solar light with intensity of 42.6 mW cm⁻² and presented in Figure 6.

The DSSC with the polymer electrolyte hybrid with 30 wt % TiO₂ nanoparticles shows a higher current density and light to electricity conversion efficiency of 2.465% compared with 1.202% of the original P(VDF-HFP) polymer electrolyte DSSC. The contrast of the data is presented in Table III. The results exhibited that the 30 wt % TiO₂ nanoparticles hybrid microporous polymer electrolyte system is better due to the higher conductive property, and the fine porous structure that can uptake more electrolyte

TABLE III
The Values of Short Current Density (J_{sc}), Open-Circuit Voltage (V_{oc}), Fill Factor, (FF), and Overall Efficiency (η), for the Cells Employing Original P(VDF-HFP) Membrane Electrolyte and TiO₂ Nanoparticles-Modified Polymer Electrolyte

TiO ₂ (wt %)	$J_{sc}/\text{mA cm}^{-2}$	V_{oc}/V	FF	$\eta/\%$
0	1.68	0.548	0.555	1.202
10	2.00	0.587	0.609	1.676
20	2.15	0.542	0.555	1.520
30	2.75	0.589	0.648	2.465
40	2.05	0.536	0.477	1.230

and the decreased crystallinity of the TiO₂ nanoparticles modified microporous polymer electrolyte is the mainly reason for the better ionic conductivity. The performance can be improved by better connecting the polymer electrolyte with TiO₂ photoanode and optimizing the electrolyte.^{25,29} Future works are carried out to optimizing the performance of the quasi-solid-state solar cells.

CONCLUSIONS

A quasi-solid-state DSSC was fabricated by phase inversion process. The experiments exhibited that the TiO₂ nanoparticles modified the P(VDF-HFP) to form more pores than the original P(VDF-HFP) porous structure, decrease the crystallinity of the polymer and increase the ionic conductivity of the microporous electrolyte. The 30 wt % TiO₂ nanoparticles modified P(VDF-HFP) microporous electrolyte membrane showed better ionic conductivity compared with the original P(VDF-HFP) electrolyte membrane. The solar to electric energy conversion efficiency of 2.465% with 30 wt % TiO₂ nanoparticles modified P(VDF-HFP) microporous electrolyte at 42.6 mW cm⁻² light intensity is better than the original DSSC, which indicates the nanoparticles optimize the microporous polymer electrolyte for the DSSC system. Further experiments are carried out to optimize the performance of the quasi-solid-state dye sensitized solar cells, such as improving the thickness of the TiO₂ photoanode, the ionic conductivity of the quasi-solid state electrolyte and the contact between the quasi-solid state electrolyte and nanocrystalline TiO₂ photoanode. In addition, other nanoparticles like SiO₂ and Al₂O₃ nanoparticles can be used in the quasi solid state polymer electrolyte system.

We acknowledge the Center of Nanoscience and Nanotechnology and the Center of Electron Microscope in Wuhan University for their sincere help.

References

1. O'Regan, B.; Grätzel, M. *Nature* 1991, 353, 737.
2. Hagfeldt, A.; Grätzel, M. *Acc Chem Res* 2000, 33, 269.
3. Hinsch, A.; Kroon, J. M.; Kern, R.; Uhlendorf, I.; Holzbock, J.; Meyer, A.; Ferber, J. *J Progr Photovolt* 2001, 9, 425.
4. Tulloch, G. E. *J Photochem Photobiol A* 2004, 164, 209.
5. Tributsch, H. *Coord Chem Rev* 2004, 248, 1511.
6. Wang, Z. S.; Kawauchi, H.; Kashima, T.; Arakawa, H. *Coord Chem Rev* 2004, 248, 1381.
7. Grätzel, M. *Prog Photovolt Res Appl* 2000, 8, 171.
8. Bach, U.; Lupo, D.; Comte, P.; Moser, J. E.; Weissörtel, F.; Salbeck, J.; Spreitzer, H.; Grätzel, M. *Nature* 1998, 395, 583.
9. Nogueira, A. F.; Durrant, J. R.; De Paoli, M. A. *Adv Mater* 2001, 13, 826.
10. Wang, P.; Zakeeruddin, S. M.; Moser, J. E.; Nazeeruddin, M. K.; Sekiguchi, T.; Grätzel, M. *Nat Mater* 2003, 2, 402.
11. Nogueira, A. F.; Longo, C.; De Paoli, M. A. *Coord Chem Rev* 2004, 248, 1455.
12. Kron, G.; Egerter, T.; Werner, J. H.; Rau, U. *J Phys Chem B* 2003, 107, 3556.
13. Tarascon, J. M.; Armand, M. *Nature* 2001, 414, 359.
14. Stephan, A. M.; Saito, Y. *Solid State Ion* 2002, 148, 475.
15. Du Pasquier, A.; Warren, P. C.; Culver, D.; Gozdz, A. S.; Amattucci, G. G.; Tarascon, J.-M. *Solid State Ion* 2000, 135, 249.
16. Tarascon, J. M.; Gozdz, A. S.; Schmutz, C.; Shokoochi, F.; Warren, P. C. *Solid State Ion* 1996, 86–88, 49.
17. Christie, A. M.; Lilly, S. J.; Staunton, E.; Andreev, Y. G.; Bruce, P. G. *Nature* 2005, 433, 50.
18. Kovac, M.; Gaberscek, M.; Grdadolnik, J. *Electrochim Acta* 1998, 44, 863.
19. Han, H. W.; Zhao, X. Z.; Liu, J. *J Electrochem Soc* 2001, 152, 1.
20. Magistris, A.; Quartaione, E.; Mustarelli, P.; Saito, Y.; Kataoka, H. *Solid State Ion* 2002, 152/153, 347.
21. Li, Z. H.; Su, G. Y.; Wang, X. Y.; Gao, D. S. *Solid State Ion* 2005, 176, 1903.
22. Croce, F.; Persi, L.; Scrosati, B.; Serraino-Fiory, F.; Plichta, E.; Hendrichson, M. A. *Electrochim Acta* 2001, 46, 2457.
23. Capiglia, C.; Saito, Y.; Kataoka, H.; Kodama, T.; Quartarone, E.; Mustarelli, P. *Solid State Ion* 2000, 131, 291.
24. Song, J. M.; Kang, H. R.; Kim, S. W.; Lee, W. M.; Kim, H. T. *Electrochim Acta* 2003, 48, 1339.
25. Grätzel, M. *J Photochem Photobiol A* 2004, 164, 3.
26. Tak, Y. H.; Kim, K. B.; Park, H. G.; Lee, K. H.; Leeb, J. R. *Thin Solid Films* 2002, 411, 12.
27. Kim, K. M.; Park, N. G.; Ryu, K. S.; Chang, S. H. *Polymer* 2002, 43, 3951.
28. Kim, Y. J.; Kim, J. H.; Kang, M. S.; Lee, M. J.; Won, J.; Lee, J. C.; Kang, Y. S. *Adv Mater* 2004, 16, 1753.
29. Han, H. W.; Liu, W.; Zhang, J.; Zhao, X. Z. *Adv Funct Mater* 2005, 15, 1940.